Journal of Sound and Vibration (2002) **253**(1), 37–56
doi:10.1006/jsvi.2001.4248, available online at http://www.idealibrary.com on IDEAL®

MYOELECTRIC RESPONSE OF BACK MUSCLES TO VERTICAL RANDOM WHOLE-BODY VIBRATION WITH DIFFERENT MAGNITUDES AT DIFFERENT POSTURES

R. Blüthner, H. Seidel and B. Hinz

Department of Occupational Health, Group AM 4.3, *Biological Effects of Vibration and Noise, Federal Institute for Occupational Safety and Health, Nöldnerstr.* 40–42, *D*-10317 *Berlin, Germany. E-mail: bluethner.ralph@baua.bund.de*

(*Accepted* 19 *October* 2001)

Back muscle forces contribute essentially to the whole-body vibration-induced spinal load. The electromyogram (EMG) can help to estimate these forces during whole-body vibration (WBV). Thirty-eight subjects were exposed to identical random low-frequency WBV (0·7, 1·0 and 1·4 m/s^{-2} r.m.s. weighted acceleration) at a relaxed, erect and bent forward postures. The acceleration of the seat and the force between the seat and the buttocks were measured. Six EMGs were derived from the right side of the m. trapezius pars descendens, m. ileocostalis lumborum pars thoracis, m. ileocostalis lumborum pars lumborum; m. longissimus thoracis pars thoracis, m. longissimus thoracis pars lumborum, and lumbar multifidus muscle. All data were filtered for anti-aliasing and sampled with 1000 Hz. Artefacts caused by the ECG in the EMG were identified and eliminated in the time domain using wavelets. The individually rectified and normalized EMGs were averaged across subjects. The EMGs without WBV exhibited characteristic patterns for the three postures examined. The coherence and transfer functions indicated characteristic myoelectric responses to random WBV with several effects of posture and WBV magnitude. A comprehensive set of transfer functions from the seat acceleration or the mean normalized input force to the mean processed EMG was presented.

The results can be used for the development of more sophisticated models with a separate control of various back muscle groups. However, the EMG–force relationship under dynamic conditions needs to be examined in more detail before the results can be implemented. Since different reflex mechanisms depending on the frequency of WBV are linked with different types of active muscle fibres, various time delays between the EMG and muscle force may be necessary.

1. INTRODUCTION

Currently, there are no reliable data on the myoelectric response to random vibration and postural myoelectric activity of back muscles. Reliable data means electromyograms (EMGs) undistorted by interference with the electrocardiogram (ECG) and related to well-defined anatomical structures. Such information will be required for a future development of sophisticated mathematical models to predict forces acting on the spine during whole-body vibration exposure (WBV). Muscle forces are assumed to contribute essentially to these forces [1, 2] and the EMG could be used to predict them provided that the EMG–force relationships can be derived for static and dynamic conditions. The close relation to anatomical structures is essential considering the advantages of anatomy-related models [3, 4]. The static, postural muscle activity is of interest for two reasons—prolonged

0022-460X/02/$35.00

sitting may be an important pathogenetic factor [5] and the constant static spinal load codetermines the health risk, if fatigue failure of the vertebral endplates is considered as an important mechanism [6].

At present, systematic data for a quantitative characterization of the EMG-response to random WBV are not available. Robertson and Griffin [7] were the first to characterize this response by a transfer function. However, these results were not related to anatomical structures and obtained with a limited frequency content of the EMG due to a high-pass filter set to 80 Hz in order to eliminate the ECG and movement artefacts. The EMG response to sinusoidal and transient vibration has been examined earlier [8, 9], but cannot be transferred directly to random vibration. The recent elaboration of a methodical approach for the elimination of artefacts, involving wavelets and digital filtering, and for the analysis of the relationship between random whole-body vibration and electromyographic responses of back muscles [10] was an important prerequisite for the systematic examination of exposure–effect relationships. The present study was aimed at the acquisition of a representative and comprehensive set of reliable data characterizing the relationship between surface EMGs associated with several important back muscles on the one hand, and random low-frequency whole-body vibration combined with different sitting postures on the other. The relationships should be described in such a way that they could be used in the future for the prediction of the EMG response to a WBV-exposure. The postural activity of back muscles with different sitting postures was also to be examined. In order to assist an application of the results, the results are presented in this paper by a comprehensive set of figures and selected numerical data in tables.

2. METHODS

2.1. SUBJECTS

Thirty-eight healthy male subjects participated as paid volunteers in the study. They were selected on the basis of a detailed anamnesis including a comprehensive assessment of the clinical state and anthropometric data used as inclusion criteria [11]. The mean values and standard deviations (in parentheses) of the age, body mass and height of the subjects were 21·6 (3·6) years, 68·0 (7·4) kg and 173·4 (5·5) cm, respectively (for more details, reference [11]).

2.2. VIBRATION EXPOSURE

The exposure simulated a selected section (65 s) of acceleration measured between the seat and the driver in z-direction of a tracked hydraulic excavator. The original exposure of 1·4 m/s^2 ISO-weighted [12] root-mean-square (r.m.s.)-value (I3) and two attenuated (-3 dB and -6 dB) levels with weighted r.m.s. values of 1·0 m/s^2 (I2) and 0·7 m/s^2 (I1) were reproduced in the laboratory by an electrohydraulic vibrator. A platform for supporting the feet, a steering wheel and a hard, anatomically formed seat without backrest were mounted on the vibrator. The subjects adopted three different postures, sitting bent-forward (B), sitting erect (E), or a relaxed driving posture (R). With posture B, the upper torso was bent forward with stretched lumbar spine, tense back muscles and with the buttocks tipped forward. Appropriate spherical control elements, side-mounted below the plane of the seat, were grasped with the hands, back of the hand ventrally directed, elbow bent. Resting on the operating elements was to be avoided. When seated upright (E), arms were crossed in front of the body, with tense back muscles and stretched lumbar spine. With

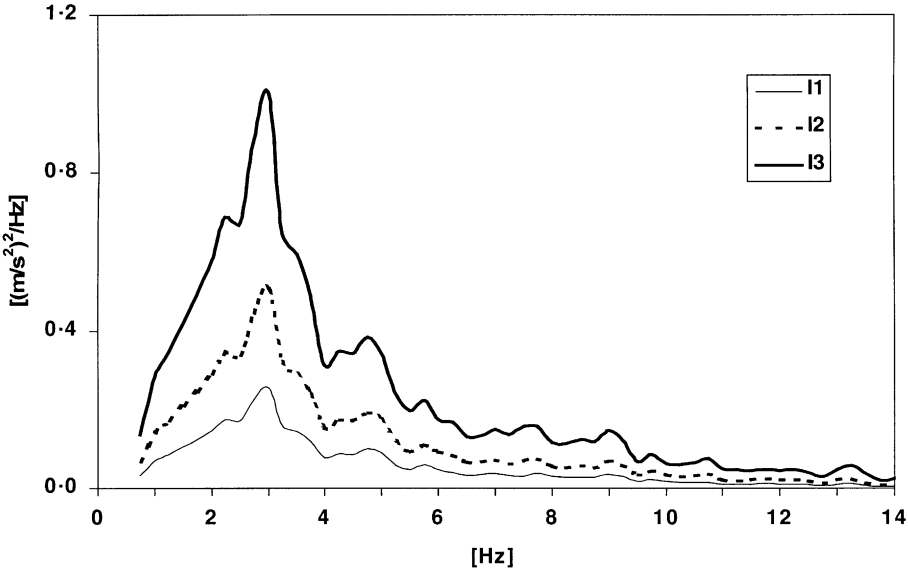

Figure 1. PSD of the seat acceleration with three intensities. I1–0·7 m/s^2 r.m.s., I2–1·0 m/s^{-2} r.m.s., I3–1·4 m/s^2 r.m.s.

the upright and subjectively comfortable posture R, the upper torso was relaxed and a steering wheel was held with both hands. The subjects controlled the postures during the exposures via videotechnique. The exposures of all subjects were nearly identical in the time and frequency domains. The power spectrum of the average acceleration exhibited at all magnitudes a similar shape with the maximum power near 3 Hz (Figure 1). More than 80 per cent of the total power was located between 1 and 9 Hz. Therefore, all calculations were restricted to this frequency range.

2.3. DATA ACQUISITION

The ECG (electrocardiogram, non-standard derivation) and six surface EMGs at the right side were acquired by bipolar derivations: EMG0—m. trapezius pars descendens, EMG1—m. ileocostalis lumborum pars thoracis, EMG2—m. ileocostalis lumborum pars lumborum; EMG3—m. longissimus thoracis pars thoracis, EMG4—m. longissimus thoracis pars lumborum, EMG5—lumbar multifidus muscle. The pickup points (Figure 2) were chosen in accordance with the results and nomenclature in references [13–15], so that as far as possible, isolated measurements could be made; that is, hardly any over layering due to other muscles was to be expected at these places. The impedance of all derivations was below 5 kΩ with 100 Hz. The electrodes were replaced if the impedance was higher. To reduce artefacts caused by electromagnetic fields and movements of the cable, pre-amplifiers (10- or 20-fold, input impedance > 1 GΩ, bandwidth from DC to > 10 kHz, common mode rejection ratio > 80 dB, input noise voltage 10 nV/$\sqrt{\text{Hz}}$) were fixed near the electrodes (impedance transformation). The EMG signals were high-pass filtered with a cut-off frequency of 10 Hz, amplified and, after an anti-aliasing filter set to 330 Hz, digitized with a sampling frequency of 1 kHz and 12 bit resolution (SCADAS II, DIFA). The accelerations of the seat in the z-direction (accelerometer Type BWH 101, Metra) and the force at the interface between the hard seat and the vibrator (three force cells Type

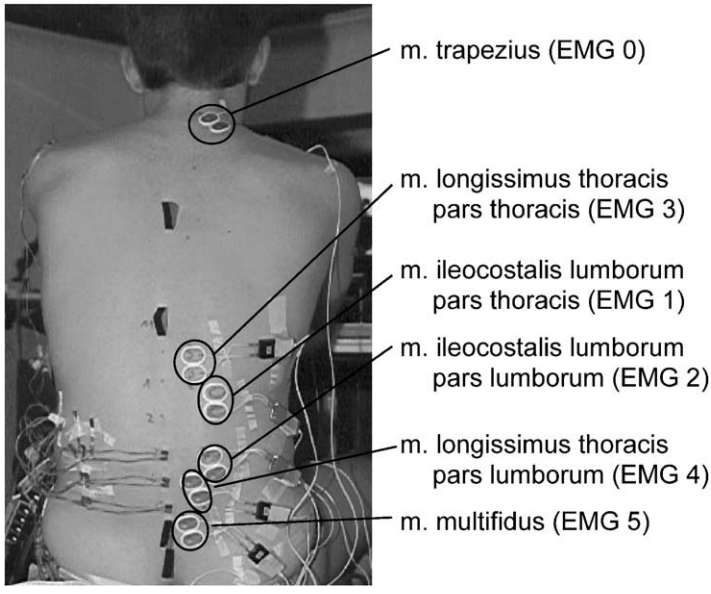

Figure 2. Back view of subject showing the arrangement of the EMG electrodes.

KWH 100, Meßelektronik Dresden) were acquired synchronously. Each registration started 1 s before and finished 1·7 s after the vibration exposure.

2.4. DATA PROCESSING

The experimental data were stored on-line in a special data format by SCADAS II. For data processing the data were transformed later into a MATLAB format. Serious methodical problems can arise with the examination of the relation between the EMG and the vibration due to disturbances. Disturbances such as an offset, the low-frequency T-wave of the ECG, and low-frequency movement artefacts, can be sufficiently reduced by high-pass filtering with a cut-off frequency around 15 Hz without a phase shift. Due to a frequency content which overlaps with EMG frequencies, artefacts caused by the QRS-complex (three distinct subsequent peaks in the ECG related to the excitation of the heart muscle and occurring with each cardiac cycle) of the ECG cannot be removed by this procedure. They can be reliably eliminated, for example, if the averaging of the EMG is performed exclusively for portions with identical parts of the exposure, these parts being located between QRS complexes. With random WBV, however, a sufficient number of identical repetitive parts of the exposure is usually not available. Therefore, even EMG segments with artefacts caused by the ECG cannot be excluded, but should rather be used in order to obtain the necessary information.

A reduction of the QRS components by high-pass filtering, e.g., by a high pass set to 80 Hz [7], could remove essential components of the EMG. Figure 3 illustrates the effects of the ECG on the surface EMGs of back muscles in the frequency domain. This effect is especially high, if the share of the ECG portion exceeds the share of the EMG portion as with EMG 4 in Figure 3. The application of wavelets to reduce the QRS artefacts was used as a promising alternative method, which does not eliminate substantial parts of the EMG (Figure 3) and can cope with the variability of the ECG-artefact.

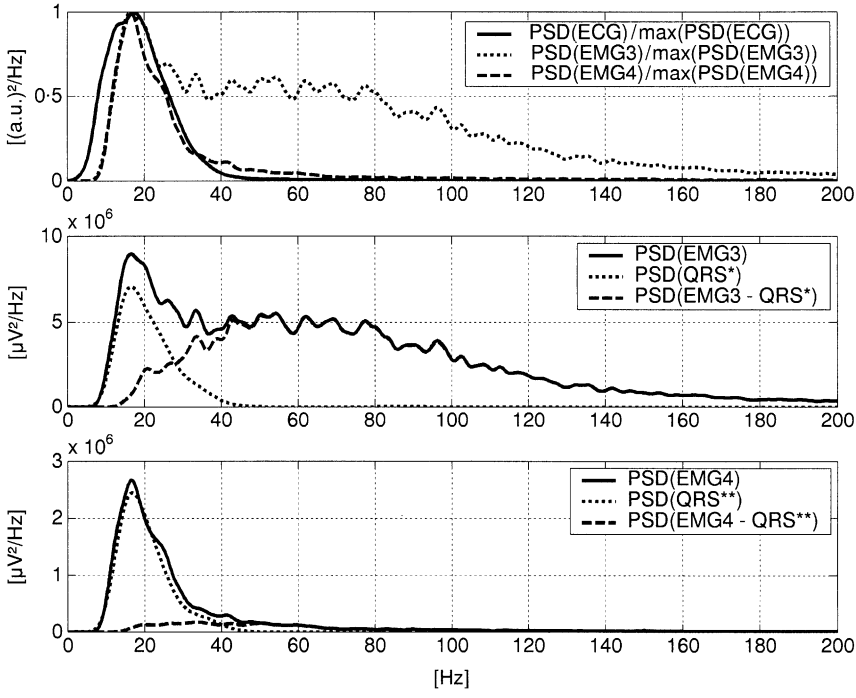

Figure 3. PSD of the ECG and two EMGs of Subject No. 176, erect posture, 1·0 m/s^2 r.m.s. Top: Normalized PSD (maximum set to 1) of the ECG, EMG3 and EMG4 without elimination of QRS complexes. Middle: PSD of the reconstructed QRS complexes detected in EMG3 (QRS*) and PSD of the EMG3 before and after elimination of QRS* complexes. Bottom: PSD of the reconstructed QRS complexes detected in EMG4 (QRS**) and PSD of the EMG4 before and after elimination of QRS** complexes.

In order to confine the subtraction of the QRS-artefacts to exactly those intervals with QRS complexes, the latter were determined in the ECG. Each EMG was decomposed into wavelet coefficients (MATLAB 5.3 and Wavelet Toolbox for use with MATLAB) characterizing different components of the signal by "approximations" and "details" at certain levels of decomposition. Subsequently, that part of the EMG containing mainly the QRS-component was reconstructed with the respective wavelet coefficients, i.e., the coefficients from the level 4 approximation of the Wavelet Toolbox, MATLAB 5.3, applied to our data. These reconstructions were subtracted from the original EMG. For each single QRS complex, 16 different mother wavelets were tested. For the artefact-reduced time series a quotient was calculated by dividing the standard deviation of every single EMG interval with a QRS artefact by the standard deviation of all artefact-free intervals of the EMG. This quotient was used as a simple decision criterion. The reconstruction with the lowest quotient was automatically selected and stored [10].

Figure 4 shows the time series of an EMG with QRS artefacts, the result of the optimally reconstructed QRS artefacts of this EMG and the artefact-reduced EMG. The example in Figure 4 illustrates the good selectivity of the procedure. All raw EMG data were treated with a high-pass filter (10 Hz), the procedure for ECG elimination, subsequent high-pass filtering (15 Hz) and normalization with respect to the r.m.s. value of the interval of the first second at the beginning of the registration with the controlled posture, but without vibration exposure.

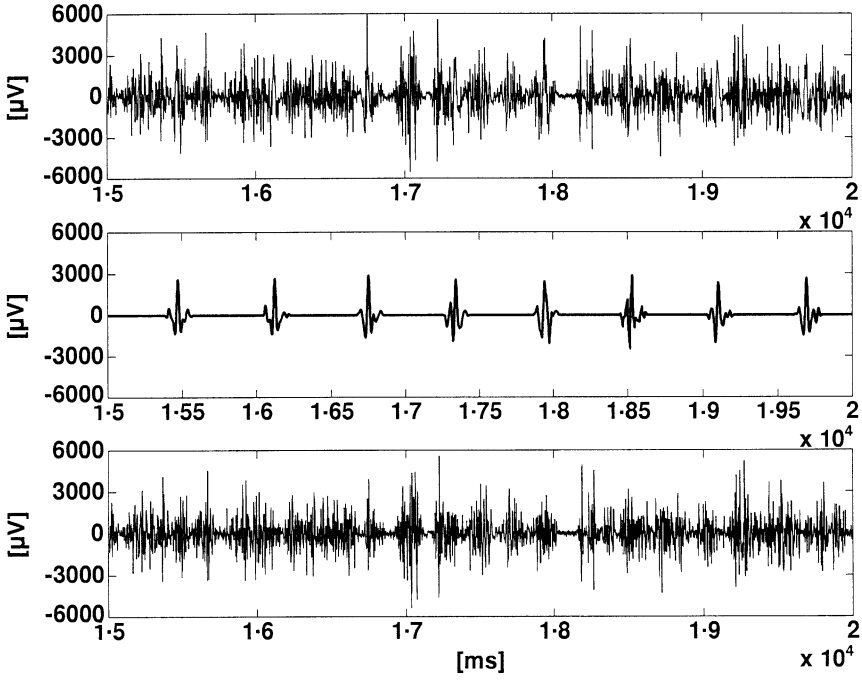

Figure 4. Elimination of the electrocardiogram from the EMG. Top: Raw EMG3 of Subject No 176, erect posture, 1·0 m/s^2 r.m.s., beginning with the 15th second of the exposure. Middle: Time series of the QRS-complexes reconstructed by optimum wavelets. Bottom: Time series of the raw EMG3 after the subtraction of the time series of the reconstructed QRS complexes.

The r.m.s. values of the non-normalized EMGs without exposure were calculated for all subjects and all postures. *t*-Tests for paired samples were used to prove the differences between r.m.s. values of each EMG arising from different sitting postures.

A systematic myoelectric reaction to the almost identical random vibration exposures was assumed for all individual subjects. Thus, a mean response in the time domain could be calculated by averaging the processed and rectified individual normalized EMGs. In order to eliminate possible outliers, the highest and lowest values at each sampling point of the 38 time series from the 38 subjects were automatically omitted instead of testing each value. A band-pass filtering was performed in order to extract the essential frequency range of the exposure between 1 and 9 Hz. This average time course of the EMG activity permitted a comparison with the average time series of the seat acceleration or the force between the seat and the buttocks.

The seat was located on three load cells arranged in the form of an isosceles triangle. The resultant force at the interface between the seat and the buttocks (input force) was calculated as the sum of the three parts reduced by the force caused by the seat. For normalizing the resultant force, after subtracting the mean value of each individual time course, i.e., the static part of the force, the dynamic part of the force was divided by its standard deviation. The mean values and standard deviations of the static and of the r.m.s. values of the dynamic parts of the force are given in Tables 1 and 2 respectively. These normalized time courses of the force (F_z) were averaged across all subjects and related to the normalized average EMG-activity. The normalization of F_z and the EMGs was used to reduce the interindividual differences before averaging.

TABLE 1

Mean values and standard deviations (in parentheses) of the static force between the seat and buttocks of 38 subjects

	Magnitude 1 (N)	Magnitude 2 (N)	Magnitude 3 (N)
Posture R	− 540·6 (75·1)	− 539·0 (76·9)	− 537·6 (75·5)
Posture E	− 582·2 (81·0)	− 582·5 (80·8)	− 582·8 (82·3)
Posture B	− 477·0 (76·1)	− 480·8 (75·3)	− 477·8 (77·2)

TABLE 2

Mean values and standard deviations (in parentheses) of the r.m.s. values of the dynamic force between the seat and buttocks of 38 subjects

	Magnitude 1 (N)	Magnitude 2 (N)	Magnitude 3 (N)
Posture R	56·2 (8·6)	78·8 (11·7)	111·4 (16.1)
Posture E	61·2 (9·2)	85·4 (12·6)	121·1 (17·2)
Posture B	54·4 (10·2)	77·8 (12·8)	111·8 (19·5)

3. RESULTS

3.1. POSTURAL EMG-ACTIVITY

Figure 5 demonstrates the mean postural EMG activity before the exposure. All EMGs exhibited a considerable between-subject variability of their r.m.s. values (in μV) arising from individual factors such as, for example, the thickness of the skin and subcutaneous tissue. The three mean r.m.s. values of each EMG were compared for the postures tested by *t*-tests for paired samples. Almost all corresponding mean values were significantly different, except for three differences—EMG0/relaxed posture versus EMG0/erect posture, EMG2/bent-forward posture versus EMG2/erect posture, and EMG4/bent-forward posture versus EMG4/erect posture. The missing difference of the EMG0 with the relaxed posture versus erect posture suggests a similar activity of the examined part of the trapezius muscle linked with the shoulder–arm position. The smaller activity of the EMG0 with the bent-forward posture may be a consequence of an increased distance between the electrodes and the muscle due to the more pronounced cervical lordosis. Except for EMG0, one common characteristic was the very low activity during the relaxed posture. It was always significantly lower than that for the two other postures and indicated a considerable relaxation of back muscles.

The differences between the erect and bent-forward postures suggested a different function of the thoracic parts of back muscles (EMG1 and EMG3) and of the multifidus muscle (EMG5) under these conditions. The former exhibited the highest activity with the erect posture, whereas the multifidus shows its highest activity with the bent-forward posture. The lumbar parts of the back muscles (EMG2 and EMG4) displayed an equally high activity with these postures. Collectively, the EMGs seem to display a characteristic pattern for each posture.

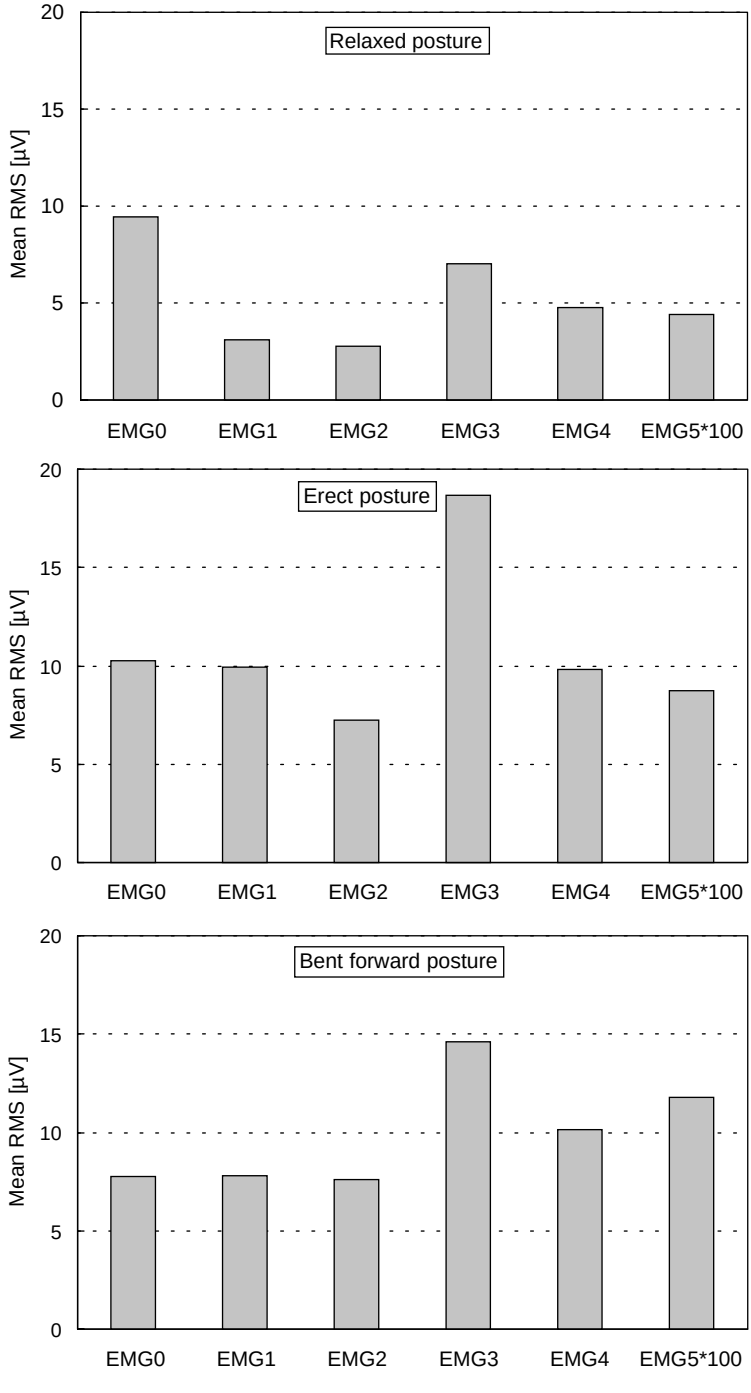

Figure 5. Postural activity of back muscles. Mean ($n = 144$) r.m.s. values of the surface electromyograms of different back muscles (EMG0–EMG5, for details see text) with three sitting postures—relaxed (top), erect (middle), and bent-forward (bottom), before the exposure to whole-body vibration.

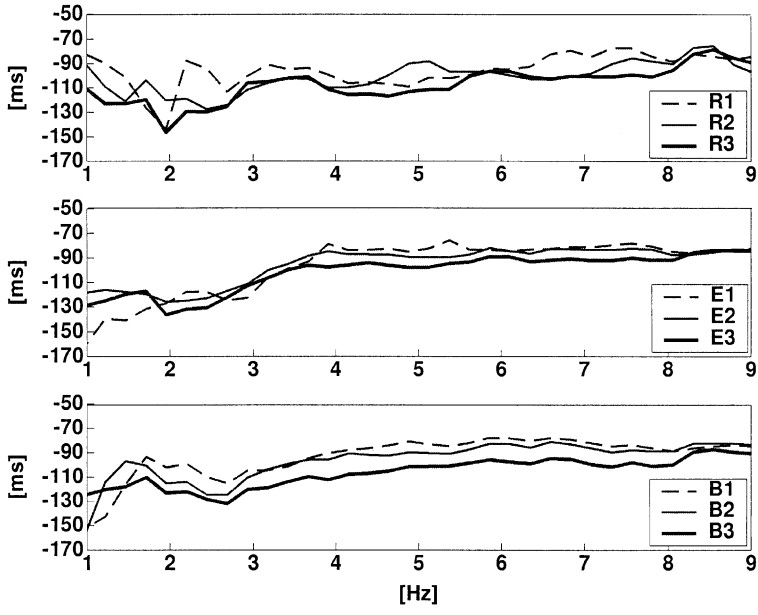

Figure 6. Time lag of the transfer function from the acceleration of the seat (1–0·7 m/s^2 r.m.s., 2–1·0 m/s^2 r.m.s., 3–1·4 m/s^2 r.m.s.) to the mean processed EMG4 with different postures (R—relaxed, E—erect, B—bent-forward).

3.2. TIME RELATION OF THE TRANSFER FUNCTION BETWEEN SEAT ACCELERATION AND NORMALIZED MEAN EMG

The coherence between the seat acceleration and the normalized EMG activity indicates the permissibility to describe the relation between both time series by a transfer function. This coherence was shown earlier with one example [10]. In general, the coherence varied between about 0·6 and 0·8 in the range 2–8 Hz. In several cases, it declined beyond this frequency range. As opposed to the conventional presentation, the phase was transformed into time differences, duly considering the period of the frequency.

For all postures (R, E, B) and all magnitudes (1, 2, 3) of the exposure, the time relations between the acceleration of the seat and the mean normalized activity of the m. longissimus thoracis pas lumborum (EMG4) and multifidus muscle (EMG5) is shown in Figures 6 and 7, respectively. There are only minor differences caused by the magnitude of WBV. The time lags appear to be larger with the high magnitude (3) and postures B and R. Different slopes below and above 4 Hz are clearly demonstrated with the erect posture (Figures 6 and 7); up to about 4 Hz, the slope corresponds to a nearly constant phase (in degrees), whilst at higher frequencies, the time relations (in ms) remain almost constant. These different time relations suggest different underlying processes such as a switching between different types of reflexes discussed earlier with respect to sinusoidal exposures [16, 17]. Similar time relations were observed with the bent-forward posture. With the relaxed posture and very low EMG activity, less distinct changes occurred.

The time relation of the transfer functions between the acceleration and the EMG4 or EMG3 were similarly shaped, but the reaction of the m. longissimus thoracis pars thoracis (EMG3) occurred earlier than that of the pars lumborum (EMG4). Figure 8 shows these time differences. A similar difference was found earlier with respect to sinusoidal exposures and transients [8].

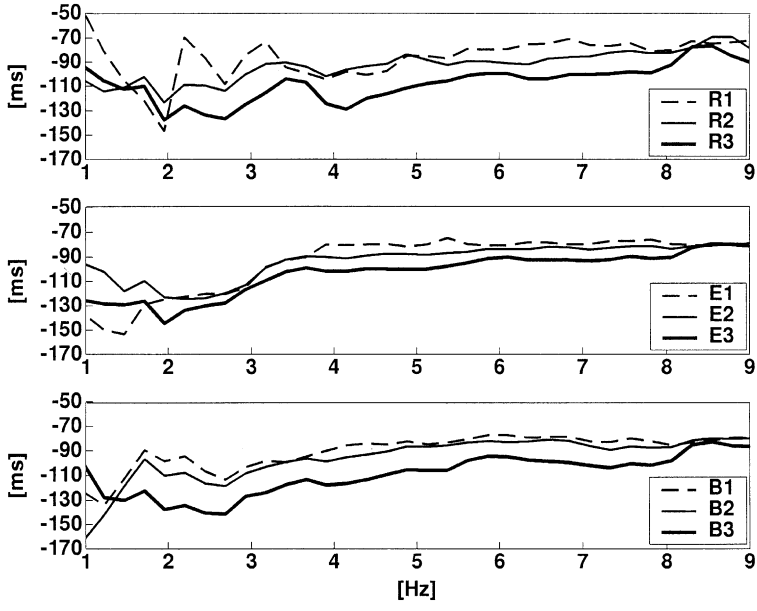

Figure 7. Time lag of the transfer function from the acceleration of the seat (1–0·7 m/s^{-2} r.m.s., 2–1·0 m/s^2 r.m.s., 3–1·4 m/s^{-2} r.m.s.) to the mean processed EMG5 with different postures (R—relaxed, E—erect, B—bent-forward).

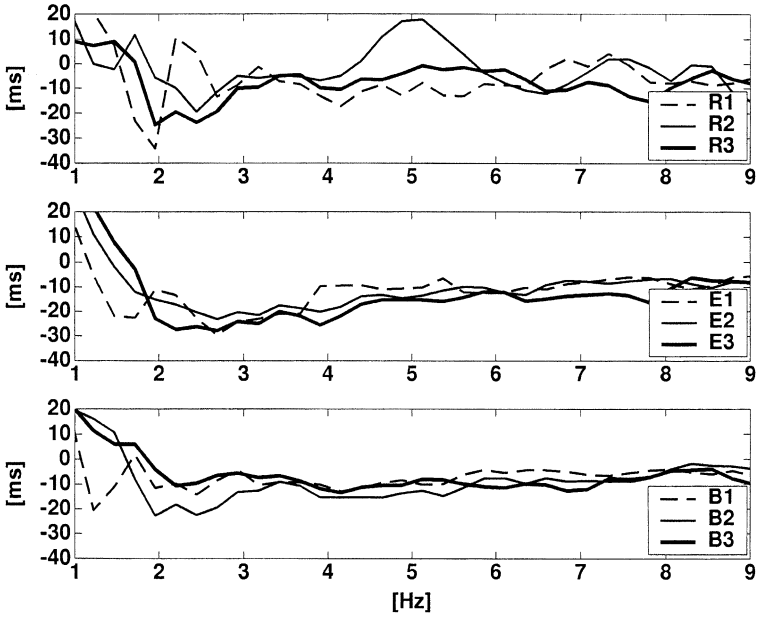

Figure 8. Difference between the time lags of the transfer functions from the acceleration of the seat (1–0·7 m/s^2 r.m.s., 2–1·0 m/s^2 r.m.s., 3–1·4 m/s^2 r.m.s.) to the mean processed EMG3 and EMG4 with different postures (R—relaxed, E—erect, B—bent-forward).

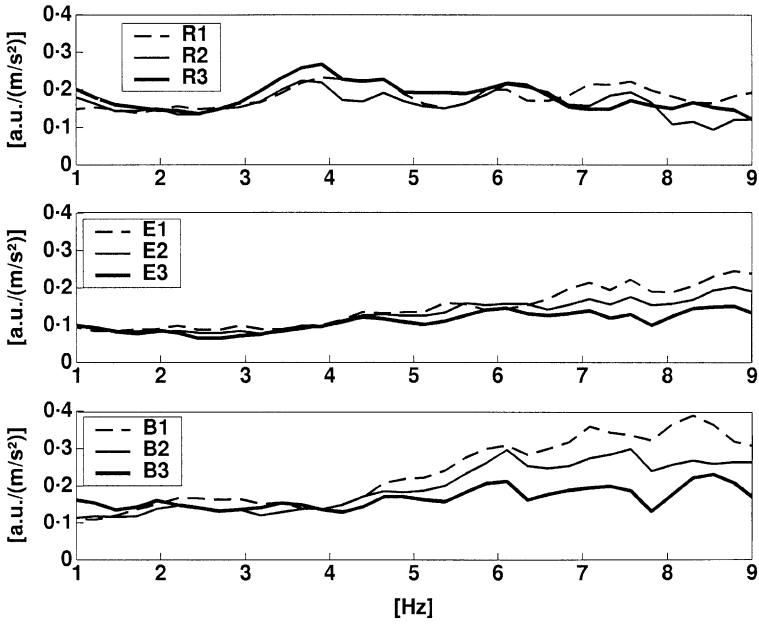

Figure 9. Modulus of the transfer function from the acceleration of the seat (1–0·7 m/s^2 r.m.s., 2–1·0 m/s^2 r.m.s., 3–1·4 m/s^2 r.m.s.) to the mean processed EMG3 in arbitrary units (a.u.) with different postures (R—relaxed, E—erect, B—bent-forward).

3.3. MODULUS OF THE TRANSFER FUNCTION BETWEEN SEAT ACCELERATION AND NORMALIZED MEAN EMG

The moduli of the transfer functions of the EMG3 and EMG4 are shown in Figures 9 and 10 respectively. Figure 11 demonstrates the modulus of the transfer function for the EMG5. No systematic differences depending on the magnitude of exposure were observed with the muscles of the lumbar region (EMG4 and EMG5). At the thoracic part of the m. longissimus thoracis (EMG3), differences were obvious (Figure 9) with the bent-forward and erect postures. In the bent-forward posture (B), the modulus increased above about 4·5 Hz and was more pronounced with the lower intensity. Similar, yet, smaller differences were observed with the erect posture. The m. ileocostalis lumborum showed an analogous reaction. At the pars thoracis of this muscle (EMG1), differences between the modulus of different magnitudes were obvious for postures E and B (Figure 12). At the lumbar part of this muscle (EMG2), no systematic differences between the different intensities at the same posture were obvious (Figure 13).

3.4. TRANSFER FUNCTION FROM THE NORMALIZED FORCE BETWEEN THE SEAT AND BUTTOCKS TO THE NORMALIZED MEAN EMG

The relation between the average acceleration of the seat and the average normalized force between the seat and the buttocks was characterised by transfer functions (Figures 14 and 15). With increasing frequency, the time lag of the force increased from almost 0 ms at 1 Hz up to about $-$ 40 ms around 7–8 Hz (Figure 14). With increasing magnitude, the time shift increased too.

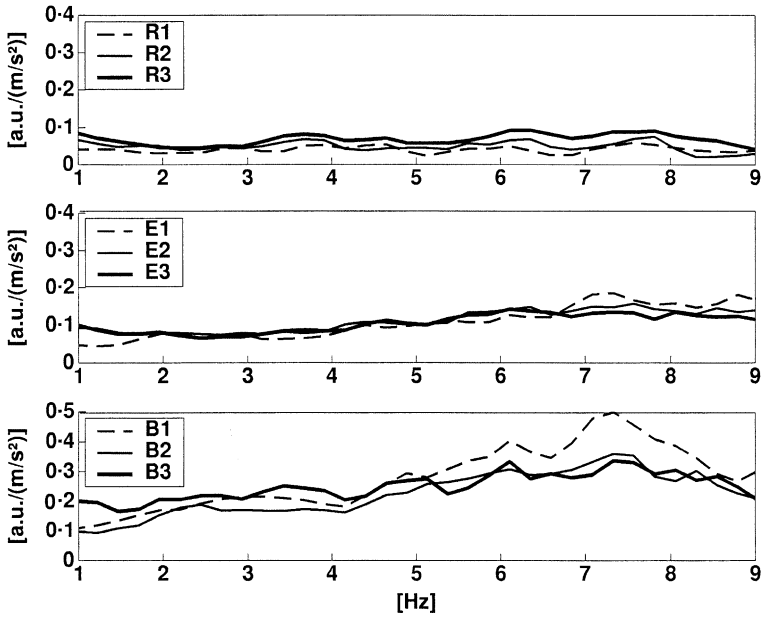

Figure 10. Modulus of the transfer function from the acceleration of the seat (1–0·7 m/s^2 r.m.s., 2–1·0 m/s^2 r.m.s., 3–1·4 m/s^2 r.m.s.) to the mean processed EMG4 in arbitrary units (a.u.) with different postures (R—relaxed, E—erect, B–bent-forward).

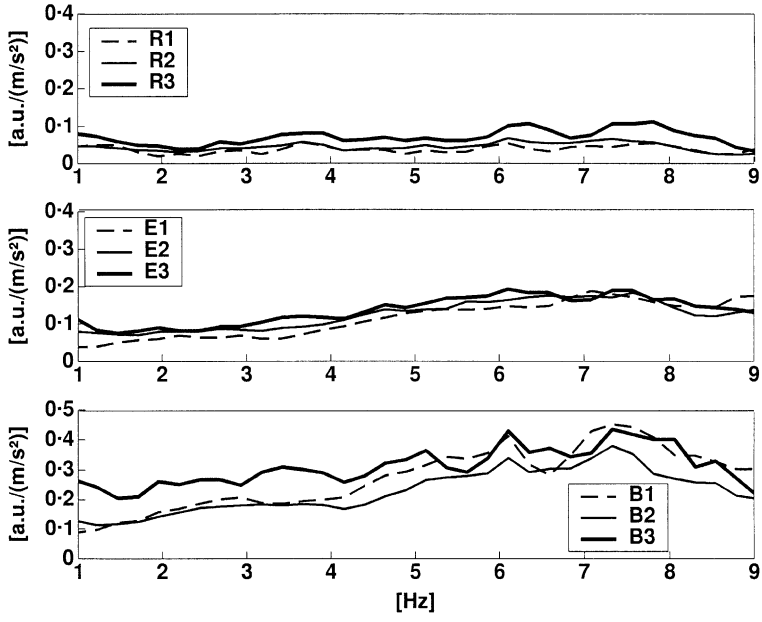

Figure 11. Modulus of the transfer function from the acceleration of the seat (1–0·7 m/s^2 r.m.s., 2–1·0 m/s^2 r.m.s., 3–1·4 m/s^2 r.m.s.) to the mean processed EMG5 in arbitrary units (a.u.) with different postures (R—relaxed, E—erect, B—bent-forward).

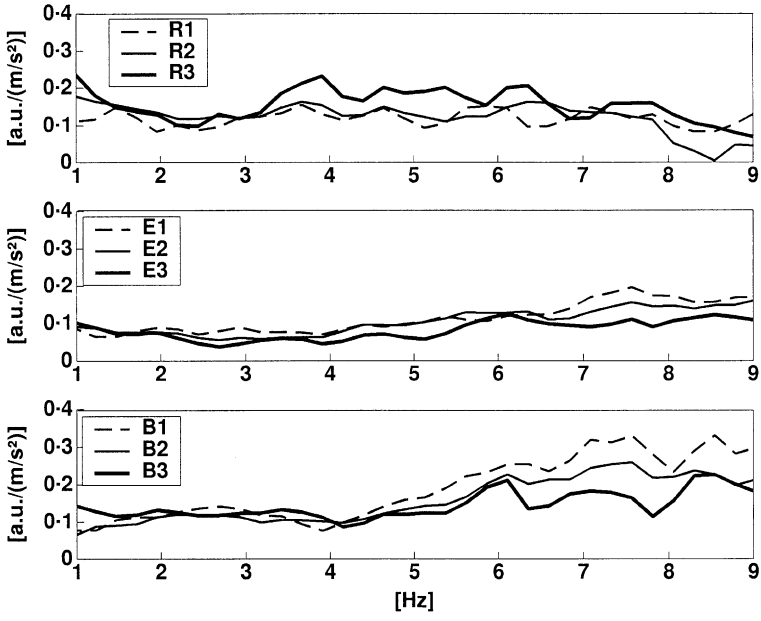

Figure 12. Modulus of the transfer function from the acceleration of the seat (1–0·7 m/s^2 r.m.s., 2–1·0 m/s^2 r.m.s., 3–1·4 m/s^2 r.m.s.) to the mean processed EMG1 in arbitrary units (a.u.) with different postures (R—relaxed, E—erect, B—bent-forward).

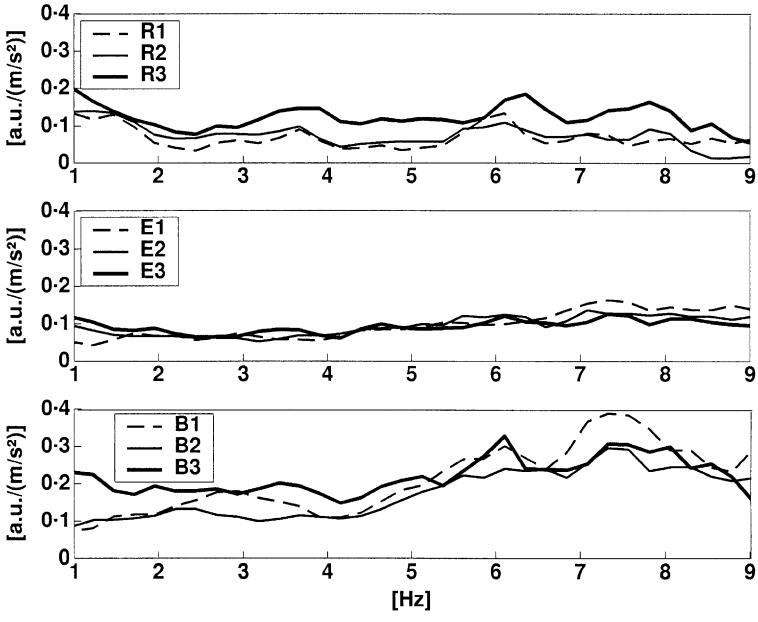

Figure 13. Modulus of the transfer function from the acceleration of the seat (1–0·7 m/s^2 r.m.s., 2–1·0 m/s^2 r.m.s., 3–1·4 m/s^2 r.m.s.) to the mean processed EMG2 in arbitrary units (a.u.) with different postures (R—relaxed, E—erect, B—bent-forward).

Since the input force was normalized, the modulus of the transfer function (from acceleration to force) decreased with an increasing magnitude of the acceleration (Figure 15). At the lowest frequency, the relations between the moduli of the different intensities of the seat acceleration were similar to the relations between the magnitudes of

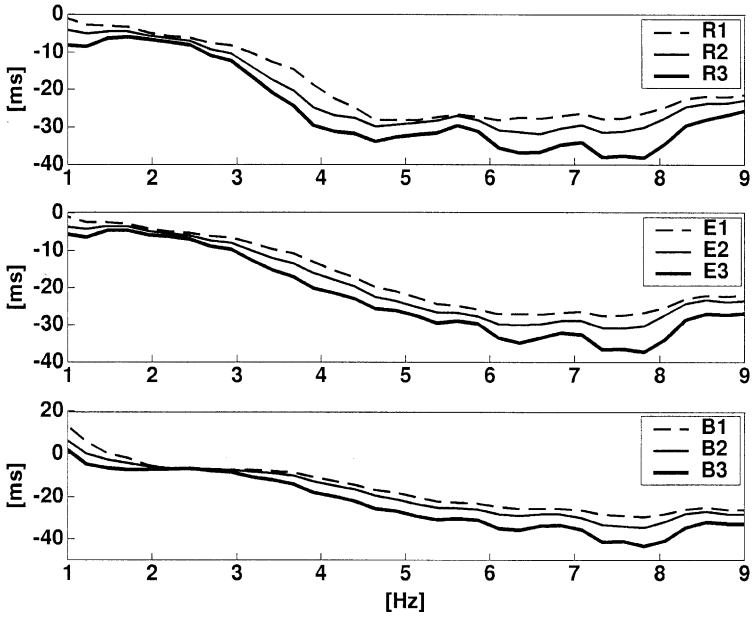

Figure 14. Time lag of the transfer function from the acceleration of the seat (1–0·7 m/s^2 r.m.s., 2–1·0 m/s^2 r.m.s., 3–1·4 m/s^2 r.m.s.) to the mean normalized force between the seat and the buttocks with different postures (R—relaxed, E—erect, B—bent-forward).

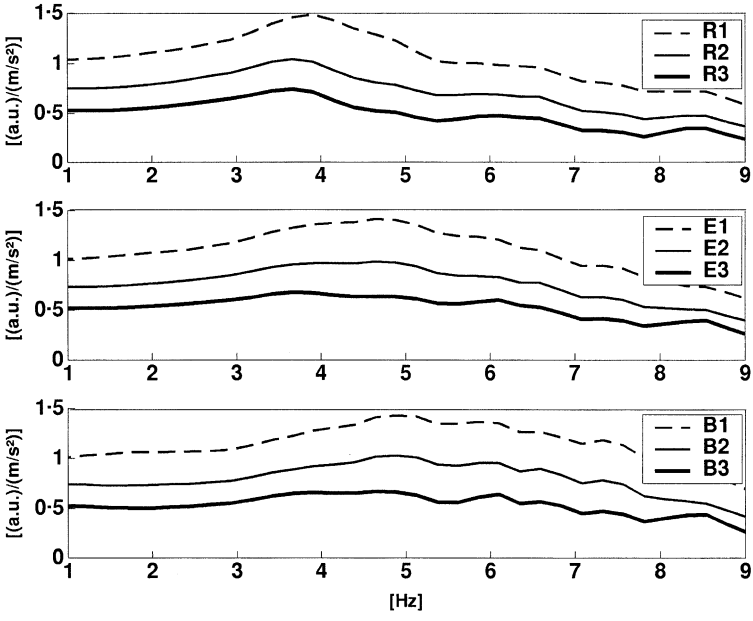

Figure 15. Modulus of the transfer function from the acceleration of the seat (1–0·7 m/s^2 r.m.s., 2–1·0 m/s^2 r.m.s., 3–1·4 m/s^2 r.m.s.) to the mean normalized force between the seat and the buttocks with different postures (R—relaxed, E—erect, B—bent-forward).

the acceleration. With the relaxed posture, maxima occurred near 4 Hz. With increasing intensity, the maximum shifted towards lower frequencies. With the erect and bent-forward postures, the frequencies of the maxima were located at about 5 Hz.

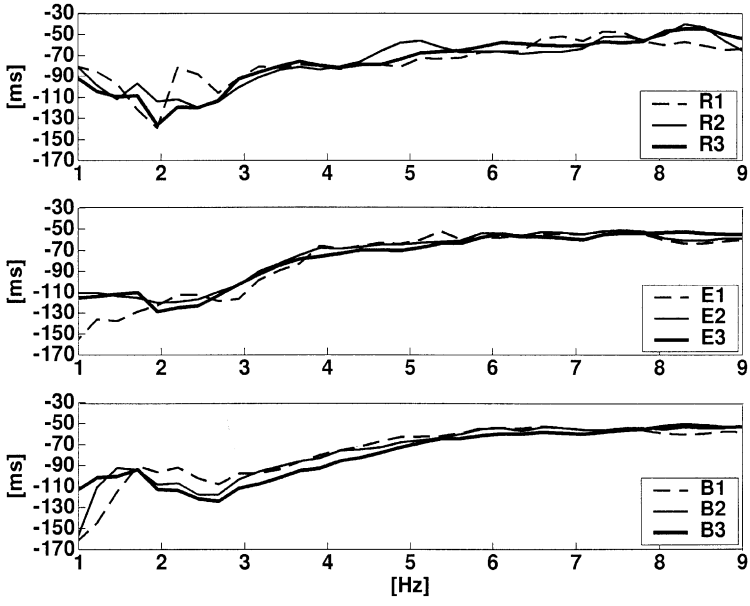

Figure 16. Time lag of the transfer function from the mean normalized force between the seat and the buttocks to the mean processed EMG4 with different postures (R—relaxed, E—erect, B—bent-forward) and magnitudes of the seat acceleration (1–0·7 m/s^2 r.m.s., 2–1·0 m/s^2 r.m.s., 3–1·4 m/s^2 r.m.s.).

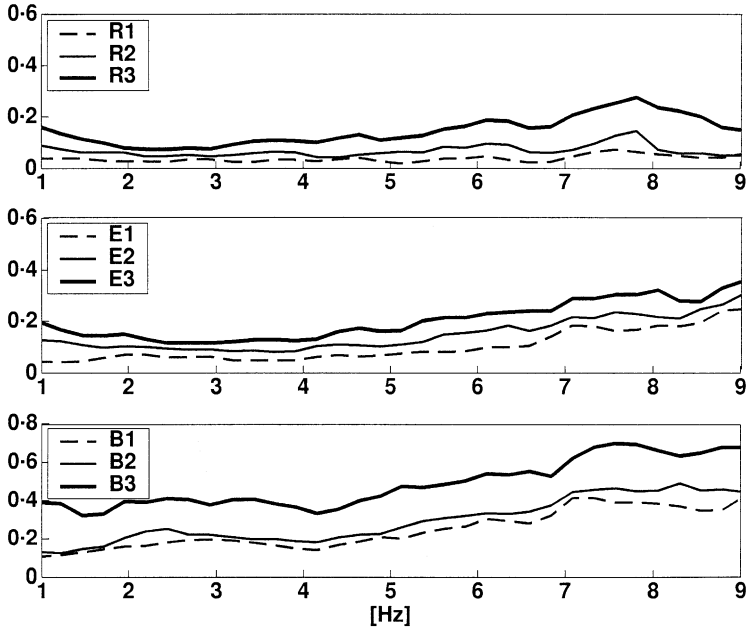

Figure 17. Modulus of the transfer function from the mean normalized force between the seat and the buttocks to the mean processed EMG4 with different postures (R—relaxed, E—erect, B—bent-forward) and magnitudes of the seat acceleration (1–0·7 m/s^2 r.m.s., 2–1·0 m/s^2 r.m.s., 3–1·4 m/s^2 r.m.s.).

The relations between the acceleration of the seat and the resultant force between the seat and the buttocks help to explain the transfer functions between the input force and the EMG when the latter are compared with transfer functions using the acceleration as input.

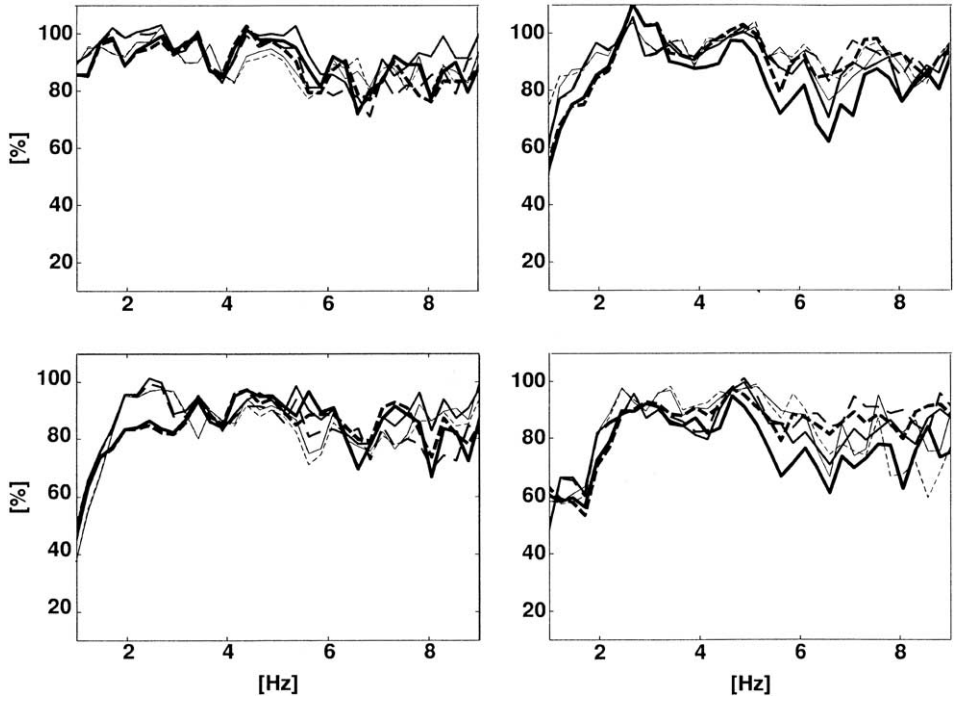

Figure 18. Relation between the predicted mean normalized EMG activity (solid lines for the prediction using the acceleration of the seat and broken lines for the prediction using the force between the seat and the buttocks) to the measured mean normalized EMG in per cent for the EMG3 (top) and the EMG4 (bottom) with three magnitudes of seat acceleration and two postures (E–erect, left; B–bent-forward, right). Key for the magnitude of exposure: thin lines 0·7 m/s^2 r.m.s., medium lines 1·0 m/s^2 r.m.s., thick lines 1·4 m/s^2 r.m.s.

As an example, the time relations between the input force and EMG4 are illustrated in Figure 16. The modulus of the same transfer functions is shown in Figure 17. The time differences are smaller than those relating the EMGs to the acceleration (cf., Figure 6), corresponding to the time relation between the acceleration and the input force (Figure 14, note the different scaling of the y-axis).

3.5. RECONSTRUCTION OF THE MEAN EMG REACTION WITH THE TRANSFER FUNCTION

It is possible to predict the EMG activity in the time domain for a seat acceleration or input force by using the relevant transfer function and inverse Fourier transform. An example of the acceptable predictability was shown earlier by a comparison of the measured and predicted EMG [10].

Another possibility to verify the quality of the reconstruction is to divide the amplitude spectrum of the reconstructed time series of the EMG activity by the amplitude spectrum of the processed measured EMG. These quotients were used to demonstrate the precision of the prediction for 24 examples (two EMGs, two postures, three magnitudes of vibration, two inputs—seat acceleration and input force) in Figure 18. The transfer function of each example shown was calculated with the data of the whole exposure time. The EMG activity was estimated for the measured acceleration or force between the seat and the buttocks by the relevant transfer-function and inverse Fourier transform. The power spectral density (PSD) of each estimated time series was divided by the corresponding PSD of the measured

EMG activity. The square roots of the quotients were multiplied by 100 to demonstrate the deviation in percentages. In Figure 18, solid lines indicate the precision for the prediction with the seat acceleration as input and broken lines indicate the prediction with the force between the seat and subject as input. The different exposure magnitudes are designated by a different line-size (magnitude 3—thick line, magnitude 2—normal line, magnitude 1—thin line). The precision was calculated for the mean EMG3 (top) and EMG 4 (bottom) in the erect posture (left) and bent-forward posture (right). The values ranged predominantly from 80 to 100 per cent. A higher precision seems to be possible by the use of the input force instead of the acceleration for frequencies above 5 Hz with the bent-forward posture.

4. DISCUSSION

4.1. POSTURAL EMG ACTIVITY

The differences between various EMGs at the same posture cannot be used as an indicator of a different mechanical postural activity, since they depend not only on the posture, but also on factors like the distance between the electrodes and skin or the size of the muscle. However, within one EMG, a comparison of the posture-related changes is possible. As an example, the high activity of the multifidus muscle with the bent-forward posture (Figure 5) could be linked with the important stabilizing function of the pelvis by this muscle. The interpretation of different, posture-related r.m.s. values of the same EMG should not neglect possible minor changes of muscle length that might have caused slightly different EMG–force relationships.

An advantage of the normalization with respect to the postural activity shall be mentioned. Since present models [18] permit the prediction of the back muscle forces with different postures, these static predicted forces, that correspond to a normalized EMG of 1, may be used as reference within a future procedure for the prediction of dynamic forces. The postural activities of back muscles contribute substantially to the internal loads acting on the lumbar spine during WBV exposures. The different posture-dependent relations of the static EMG activities should be kept in mind when the normalized EMG responses to WBV are compared—a relative doubling of the activity with the relaxed posture means much less force than a relative doubling of the activity during the erect posture.

4.2. TRANSFER FUNCTION

If the muscles respond systematically to random WBV, the transfer function can be used to characterize the exposure–effect relationship. Due to its higher frequency content, the raw EMG is not a suitable response measure. The data processing of the EMG applied in this paper—filtering, artefact elimination, rectification, normalization and averaging across subjects—led to a signal that was assumed to represent the typical mean response and could be related to the input acceleration, although considerable "smoothing" of individual features can happen. This processed EMG also offers a better possibility to predict a mechanical muscle activity in the future, because this prediction requires a similar treatment of the EMG signal. So far the between-subject variability of the transfer functions remains an open question, since the necessary number of repeated measurements within one subject was not available. The latter would also be a prerequisite for testing statistical differences between transfer functions for different conditions. It cannot be assumed that the WBV exposure can explain completely the myoelectric activity, since parts of the overall

activity may be controlled by higher control loops like the pattern generator [19] or voluntary control.

The time lag of the transfer functions suggests the change of the reflex type and also the reflex time near the whole-body resonance postulated for sinusoidal and transient WBV [16, 17]. The reflex type is related to the type of the muscle fibre activated by stretch [20] caused by the relative movements in the body, with the latter induced by the passive body response. Different electromechanical delays may be expected below and above the resonance, because of the different electromechanical delays for slow and fast fibres. A better estimation of the time course of the muscle force based on the myoelectric activity could be expected, if the type of reflex is given proper consideration. While the time lag of the transfer function from the acceleration to the EMG4 increased with the magnitude 3 (Figure 6), similar differences were not obvious with the force as input (Figure 16). The time relations between the seat acceleration and the input force (Figure 14) offer one possible explanation. The input force reflects some interaction between vibration and the human body. Therefore, one can assume this force to be more closely related to the internal stimulus, the passive body response mechanism, that probably elicits the reflex-like muscular reaction. The transfer functions from the seat acceleration to the input force indicate some non-linearity as a shift of the resonance peak and a phase changing with the WBV-magnitude (cf., Figure 14). If this non-linear behaviour would be linked with the internal reflex stimulus, the input force as a result of the interaction between the passive-body response and muscular reaction should exhibit less variable time relations to the EMG response than the seat acceleration.

Up to about 4·5 Hz the extent of the mean normalized EMG response per unit of the acceleration of the seat was nearly constant for the erect posture. In the same frequency range, the moduli of the transfer function were independent of the magnitude of the exposure (Figures 9–13, middle). Systematic differences were obvious above about 5 Hz for the thoracic parts of back muscles (Figures 9 and 12), but not for the lumbar parts (Figures 10, 11 and 13). The response of EMG3 and EMG1 declined with increasing magnitude (Figures 9 and 12). Two explanations are conceivable—either the extent of the internal stimulus eliciting the EMG response decreased due to underlying non-linear biodynamics, or the neural mechanism of the reflex-loop was affected. This diminishing response above 5 Hz together with the mechanical low-pass filter characteristics of the muscle [21, 22] will be important for future models that reflect appropriately the actual muscular response.

4.3. RECONSTRUCTION

The examples in Figure 18 show that the transfer function is a suitable instrument to predict the muscle response to random vibration. The mean precision of the estimation in the relevant frequency range was about 90 per cent in all cases. With the bent-forward posture, the precision of the estimation was somewhat better, if the input force in the frequency range above 5 Hz was used for the transfer function. Within the precision described, it should be possible to estimate an average normalized electrical muscle activity without an experimentally derived EMG.

5. CONCLUSIONS

The relations between the myoelectric response of back muscles and random whole-body vibration of different magnitudes and with different postures were quantitatively characterized by transfer functions based on averaged EMG time series. The extent to

which these functions are significantly different remains unresolved. A statistical comparison between the different transfer functions would require additional experimental data. The results could be used to predict an average EMG response under similar conditions. For this purpose, it is recommended to choose the function obtained under a condition nearest to that of the prediction. These results could be applied in models that include the possibility of a separate control of various back muscle groups, thus enabling the mean typical back muscle activity to be taken into account without the need to examine the EMG response. However, the EMG–force relationship under dynamic conditions needs to be examined in more detail before the results can be implemented this way.

ACKNOWLEDGMENTS

This research was supported by the European Commission under the BIOMED 2 concerted action BMH4-CT98-3251 (Vibration Injury Network).

REFERENCES

1. H. SEIDEL, R. BLÜTHNER and B. HINZ 1986 *International Archives of Occupational and Environmental Health* **58**, 207–223. Effects of sinusoidal whole-body vibration on the lumbar spine: the stress–strain relationship.
2. M. A. ADAMS and P. DOLAN 1995 *Clinical Biomechanics* **10**, 3–19. Recent advances in lumbar spinal mechanics and their clinical significance.
3. B. BUCK, ST. PANKOKE and H. P. WÖLFEL 1997 *Lateralsymmetrisches Modell der Lendenwirbelsäule zur Berechnung dynamischer Bandscheibenkräfte* (*Schlußbericht*). Bremerhaven: Wirtschaftverlag NW.
4. H. SEIDEL and M. J. GRIFFIN 2001 *Clinical Biomechanics* **16**, S3-S7. Modelling the response of the spinal system to whole-body vibration and repeated shock.
5. J. SANDOVER 1981 *Research Report No DHS* 402, *Department of Human Sciences*, *University of Technology*, *Loughborough*. Vibration, posture and low-back.
6. H. SEIDEL, R. BLÜTHNER, B. HINZ and M. SCHUST 1998 *Journal of Sound and Vibration* **215**, 723–741. On the health risk of the lumbar spine due to whole-body vibration—theoretical approach, experimental data and evaluation of whole-body vibration.
7. C. D. ROBERTSON and M. J. GRIFFIN 1989 *I.S.V.R. Technical Report* 184, *Institute of Sound and Vibration Research*, *University of Southampton Laboratory*. Southampton: Human Factors Research Unit. Studies of the electromyographic response to whole-body vibration.
8. R. BLÜTHNER, B. HINZ, G. MENZEL and H. SEIDEL 1993 *International Journal of Industrial Ergonomics* **12**, 49–59. Back muscle response to transient whole-body vibration.
9. R. BLÜTHNER, H. SEIDEL and B. HINZ 1998 *Journal of Low Frequency Noise*, *Vibration and Active Control* **17**, 215–226. Timing of back muscles during whole-body vibration with transients—its significance for the internal spinal load.
10. R. BLÜTHNER, H. SEIDEL and B. HINZ 2001 *Clinical Biomechanics* **16**, S25–S30. Examination of the myoelectric activity of back muscles during random vibration—methodical approach and first results.
11. H. SEIDEL, R. BLÜTHNER, B. HINZ and M. SCHUST 1997 *Schriftenreihe der Bundesanstalt für Arbeitsschutz und Arbeitsmedizin Fb* 777. Bremerhaven: Wirtschaftsverlag NW. Stresses in the lumbar spine due to whole-body vibration containing shocks.
12. ISO 2631/1-1985(E). *International Standard Evaluation of human exposure to whole-body vibration. Part* 1: *general requirements*. 1985-05-15, Geneva: International Organization for Standardization; first edition.
13. J. E. MACINTOSH, F. VALENCIA, N. BOGDUK and R. R. MUNRO 1986 *Clinical Biomechanics* **1**, 196–204. The morphology of the human lumbar multifidus.
14. J. E. MACINTOSH and N. BOGDUK 1987 *Spine* **12**, 658–668. The morphology of the lumbar erector spinae.
15. J. E. MACINTOSH and N. BOGDUK 1991 *Spine* **16**, 783–792. The attachments of the lumbar erector spinae.

16. R. BLÜTHNER, H. SEIDEL and B. HINZ 1997 in *UK Group Meeting on Human Response to Vibration*, 61–72, 17–19 September, Southampton: Human Factors Research Unit, Institute of Sound and Vibration Research, University of Southampton. Can reflex-mechanism explain the timing of back muscles during sinusoidal whole-body vibration and transients?
17. R. BLÜTHNER 1998 *Sicher ist sicher* **5**, 223–228. Skelettbelastung durch Schwingungseinwirkung.
18. ST. PANKOKE, J. HOFMANN and H. P. WOELFEL 2000 *Schriftenreihe der Bundesanstalt für Arbeitsschutz und Arbeitsmedizin Fb* 885. Development of a model for calculating forces in the lumbar spine (German). Bremerhaven: Wirtschaftsverlag NW.
19. S. GRILLNER and P. WALLEN 1985 *Annual Review of Neuroscience* **8**, 233–261. Central pattern generators for locomotion with special reference to vertebrates.
20. P. ROMAIQUERE, J.-P. VETTEL, J.-P. AZULAY and S. PAGNI 1991 *Journal of Physiology* **444**, 645–667. Differential activation of motor units in the wrist extensor muscles during the tonic vibration reflex in man.
21. J. C. HOUK, W. Z. RYMER 1981 in *Handbook of physiology*, V. B. Brooks (editor) Vol. 2, Part 1, 257–323. Baltimore, MD: Waverly Press. Neuronal control of muscle length and tension.
22. P. M. RACK 1981 in *Handbook of physiology*, V. B. Brooks (editor), Vol. 2, Part 1, 229–256. Baltimore, MD: Waverly Press. Limitations of somasensory feedback in control of posture and movement.

APPENDIX A: NOMENCLATURE

B	bent-forward posture
E	erect posture
ECG	electrocardiogram
EMG	electromyogram
EMG0	EMG of the m. trapezius
EMG1	EMG of the m. ileocostalis lumborum pars thoracis
EMG2	EMG of the m. ileocostalis lumborum pars lumborum
EMG3	EMG of the m. longissimus thoracis pars thoracis
EMG4	EMG of the m. longissimus thoracis pars lumborum
EMG5	EMG of the lumbar multifidus muscle
I1	magnitude 1 (0·7 ms^{-2} r.m.s. weighted acceleration)
I2	magnitude 2 (1·0 ms^{-2} r.m.s. weighted acceleration)
I3	magnitude 3 (1·4 ms^{-2} r.m.s. weighted acceleration)
PSD	power spectral density
QRS	three distinct subsequent peaks in the ECG
R	relaxed posture
r.m.s.	root mean square
WBV	whole-body vibration